J. Plasma Physics (2010), *vol.* 76, *part* 6, *pp.* 893–901. © Cambridge University Press 2010
doi:10.1017/S0022377810000486

Nonlinear electromagnetic wave interactions in Hall–MHD plasmas

DASTGEER SHAIKH[1] and P. K. SHUKŁA[2]

[1]Department of Physics and Center for Space Physics and Aeronomic Research (CSPAR), University of Alabama at Huntsville, Huntsville, AL 35805, USA
(dastgeer.shaikh@uah.edu)

[2]Institut für Theoretische Physik, Fakultät für Physik und Astronomie, Ruhr-Universität Bochum, D-44780 Bochum, Germany
(ps@tp4.rub.de)

(Received 1 July 2010, revised 3 July 2010 and accepted 4 July 2010, first published online 2 September 2010)

Abstract. We have developed a massively parallelized fully three-dimensional (3D) compressible Hall–magnetohydrodynamic (MHD) code to investigate inertial range electromagnetic wave cascades and dissipative processes in the regime, where characteristic length scales associated with plasma fluctuations are smaller than ion gyroradii. Such regime is ubiquitously present in the solar wind and many other collisionless space plasmas. Particularly, in the solar wind, the high time resolution databases depict a spectral break near the end of the 5/3 spectrum that corresponds to a high-frequency regime where the electromagnetic turbulent cascades cannot be explained by the usual MHD models. This refers to a second inertial range, where turbulent cascades follow a $k^{-7/3}$ (where k is a wavenumber) spectrum in which the characteristic electromagnetic fluctuations evolve typically on kinetic Alfvén time scales. In this paper, we describe results from our 3D compressible Hall–MHD simulations that explain the observed $k^{-7/3}$ spectrum in the solar wind plasma, energy cascade, anisotropy, and other spectral features.

1. Introduction

Electromagnetic (EM) fluctuations in many space and astrophysical processes comprise a multitude of time and length scales that are smaller than the ion gyroperiod (Ω_{ci}^{-1}, where Ω_{ci} is the ion gyrofrequency) and the ion gyroradius, respectively. These EM fluctuations cannot be described by the usual magnetohydrodynamic (MHD) models [8, 13–18, 24–26]. Typically, the reconnection of magnetic field lines near the solar corona [1], Earth's magnetosphere, and in many laboratory plasma devices [2] are other avenues where collisionless or kinetic processes call for the inclusion of finite Larmor radius effects in the standard MHD model. In particular, in the context of the solar wind plasma, higher time resolution databases identify a spectral break near the end of the MHD inertial range spectrum that corresponds to a high-frequency ($>\Omega_{ci}$) regime where turbulent cascades *cannot* be explained by Alfvénic cascades. This refers to a secondary inertial range where turbulent cascades follow a $k^{-7/3}$ (where k is a wavenumber) spectrum in which the characteristic fluctuations evolve typically on the kinetic Alfvén time scales. The

https://doi.org/10.1017/S0022377810000486 Published online by Cambridge University Press

onset of the second or the kinetic Alfvén inertial range still eludes our understanding of solar wind fluctuations [9]. The mechanism leading to the spectral break has been thought to be either mediated by the kinetic Alfvén waves (KAWs), or damping of ion cyclotron waves, or dispersive processes, or other implicit nonlinear interactions associated with kinetic effects in the solar wind plasma [5–7, 12]. Motivated by these issues, we have developed three-dimensional (3D), time-dependent, compressible, non-adiabatic, driven, and fully parallelized Hall–MHD simulations to investigate turbulent spectral cascades in collisionless space plasmas.

In this paper, we describe some results from our 3D Hall–MHD code. The manuscript is organized in the following fashion. We begin by describing the underlying Hall–MHD model in Sec. 2. The results of nonlinear simulations are presented in Sec. 3. Section 4 deals with the spectra in KAW regime of our Hall–MHD plasma. In Sec. 5, we discuss anisotropic cascades of EM fluctuations. Our conclusions are contained in Sec. 6.

2. Two-fluid model of the Hall–MHD plasma

The underlying model, in our simulations, is based on the two fluid Hall–MHD description of the magnetized plasma composed of electrons and ions. In the high-frequency regime, $\omega > \Omega_{ci}$, the inertialess electrons contribute to the electric field which is dominated essentially by the Hall term corresponding to $\mathbf{J} \times \mathbf{B}$ force. The latter, upon substituting in the ion momentum equation, modifies the ion momentum, the magnetic field and total energy in a manner to introduce a high-frequency ($\omega > \Omega_{ci}$) and short scale ($k_\perp \rho_L > 1$, where ρ_L is ion gyroradius) plasma motions. The characteristic length scales (k^{-1}) associated with the plasma motions are smaller than ion gyroradius (ρ_L). The quasi-neutral solar wind plasma density (ρ), velocity ($\mathbf{U}$), magnetic field ($\mathbf{B}$), and total pressure ($P = P_e + P_i$) fluctuations can then be cast into a set of the Hall–MHD equations, given by

$$\frac{\partial \rho}{\partial t} + \nabla \cdot (\rho \mathbf{U}) = 0, \tag{2.1}$$

$$\rho \left(\frac{\partial}{\partial t} + \mathbf{U} \cdot \nabla \right) \mathbf{U} = -\nabla P + \frac{1}{c} \mathbf{J} \times \mathbf{B}, \tag{2.2}$$

$$\frac{\partial \mathbf{B}}{\partial t} = \nabla \times \left(\mathbf{U} \times \mathbf{B} - d_i \frac{\mathbf{J} \times \mathbf{B}}{\rho} \right) + \eta \nabla^2 \mathbf{B}, \tag{2.3}$$

$$\frac{\partial e}{\partial t} + \nabla \cdot \left(\frac{1}{2} \rho U^2 \mathbf{U} + \frac{\gamma}{\gamma - 1} \frac{P}{\rho} \rho \mathbf{U} + \frac{c}{4\pi} \mathbf{E} \times \mathbf{B} \right) = 0, \tag{2.4}$$

where the notations are standard and

$$e = \frac{1}{2} \rho U^2 + \frac{P}{(\gamma - 1)} + \frac{B^2}{8\pi}$$

is the total energy of our uniform magnetized plasma. All the dynamical variables are functions of three space and a time, i.e. (x, y, z, t), co-ordinates. Equations (2.1)–(2.4) are normalized by the typical length ℓ_0 and time $t_0 = \ell_0 / v_0$ scales in our simulations, where $v_0 = B_0/(4\pi\rho_0)^{1/2}$ is the Alfvén speed, such that $\bar{\nabla} = \ell_0 \nabla, \partial/\partial \bar{t} = t_0 \partial/\partial t, \bar{\mathbf{U}} = \mathbf{U}/v_0, \bar{\mathbf{B}} = \mathbf{B}/v_0(4\pi\rho_0)^{1/2}, \bar{P} = P/\rho_0 v_0^2, \bar{\rho} = \rho/\rho_0$. The parameters μ and η

https://doi.org/10.1017/S0022377810000486 Published online by Cambridge University Press

correspond, respectively, to the ion-electron viscous drag term and the magnetic field diffusivity. While the viscous drag modifies the dissipation in the plasma momentum in a nonlinear manner, the magnetic diffusion damps the small-scale magnetic field fluctuations linearly. The dimensionless parameter in the magnetic field (2.3) i.e. the ion skin depth $\bar{d}_i = d_i/\ell_0, d_i = c/\omega_{pi}$ is associated with the Hall term. This means the ion inertial scale length (d_i) is a natural or an intrinsic length scale present in the Hall–MHD model, which accounts for finite Larmour radius effects corresponding to high-frequency oscillations in $kd_i > 1$ regime. Clearly, Hall forces dominate the magnetoplasma dynamics when $1/\rho(\mathbf{J} \times \mathbf{B}) > \mathbf{U} \times \mathbf{B}$ term in (2.3) which in turn introduces time scales corresponding to the high-frequency plasma fluctuations in $kd_i > 1$ regime. Furthermore, our model includes a full energy equation (see (2.4)), unlike an adiabatic equation of state that relates the pressure and density in a classical way. The use of the energy equation enables us to study a self-consistent evolution of turbulent heating resulting from nonlinear energy cascades in the solar wind plasma.

In the linear regime, the Hall–MHD equations admit a dispersion relation [4],

$$\left(\omega^2 - k_z^2 V_A^2\right) D_m(\omega, \mathbf{k}) = \omega^2 \left(\omega^2 - k^2 V_s^2\right) k_z^2 k^2 \frac{V_A^4}{\omega_{ci}^2},$$

which exhibits coupling among the high-frequency electron whistlers [28], KAWs, fast and slow magnetosonic waves given by the solutions of

$$D_m(\omega, \mathbf{k}) = \omega^4 - \omega^2 k^2 \left(V_A^2 + V_s^2\right) + k_z^2 k^2 V_A^2 V_s^2 = 0,$$

where ω is the frequency, $\mathbf{k}$ ($= \mathbf{k}_\perp + k_z \hat{\mathbf{z}}$ is the wave vector, the subscripts $\perp$ and z denote the components across and along the external magnetic fields $B_0\hat{\mathbf{z}}$, V_A and V_s are the Alfvén and effective sound speeds, respectively) is the EM ion-cyclotron Alfvén (EMICA) waves. The warm Hall–MHD plasma thus supports a great variety of waves having different wavelengths (comparable to the ion skin depth associated with the Hall drift, the ion sound gyroradius associated with the electron pressure and the perpendicular ion inertia/ion polarization drift).

3. Results from numerical simulations

The EM wave fluctuations are initialized by using a uniform isotropic random spectral distribution of Fourier modes concentrated in a smaller band of lower wavenumbers ($k < 0.1k_{max}$). While spectral amplitude of the EM fluctuations is random for each Fourier coefficient, it follows a certain initial spectral distribution proportional to $k^{-\alpha}$, where α is an initial spectral index. The spectral distribution set up in this manner initializes random scale EM turbulent fluctuations. A constant background magnetic field is included along the z direction to deal primarily with the large-scale or background solar wind magnetic field. EM turbulent fluctuations in our simulations are driven either at the lowest Fourier modes or evolve freely under the influence of self-consistent dynamics described by the set of (2.1)–(2.4). The inertial range spectral cascades in the either cases lead to the nearly identical turbulent spectra. We have further carried out simulations for a range of various parameters and spectral distributions to ensure the validity of our codes and the physical results. Since the initial energy is localized in the large-scale fluctuations, the latter drive turbulent processes through migration of energy towards relatively small

https://doi.org/10.1017/S0022377810000486 Published online by Cambridge University Press

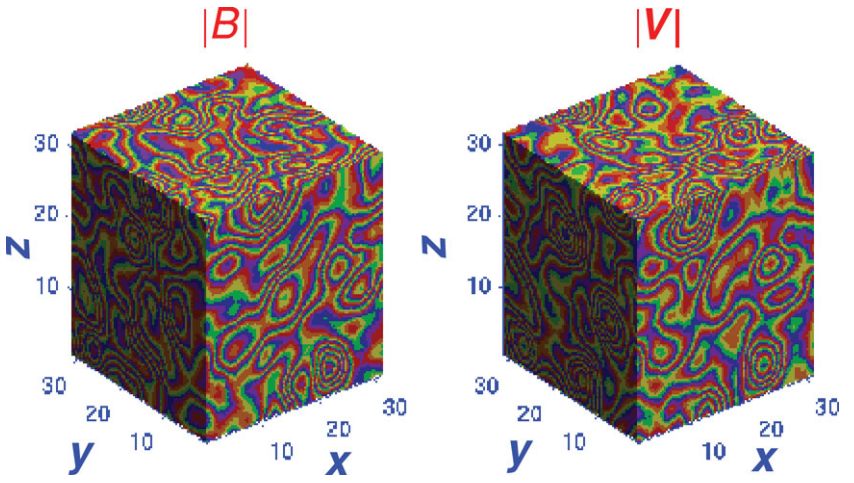


Figure 1. (Colour online) Three-dimensional structures of the magnetic, velocity, and current fields in the Hall–MHD turbulence. The turbulent equipartition between velocity and magnetic field leads to almost similar large-scale structures in the two fields, while current is more intermittent. The magnitude of the constant contours range from −0.02 to 0.02.

scales. Consequently, larger eddies transfer their energy to smaller ones through a forward cascade. During the forward cascade process, each Fourier modes in the inertial range spectrum obey the vector triad constraints imposed by the wave number selection rule, $\mathbf{k}+\mathbf{p}=\mathbf{q}$. These nonlinear interactions involve the neighboring Fourier components $(\mathbf{k},\mathbf{p},\mathbf{q})$ that are excited in the local inertial range turbulence. The mode structures associated with the nonlinear evolution of magnetic, velocity, and current fields are depicted in Fig. 1. Evidently, the presence of the guide magnetic field along the $\hat{z}$ direction makes the EM fluctuations anisotropic (i.e. disparity in the length scales along and across the mean magnetic field), while the length scales in the perpendicular plane, i.e. xy-plane, exhibit nearly isotropic evolution.

The evolution of the kinetic and magnetic helicities is shown in Fig. 2. While the kinetic and magnetic energies are ideal invariants of the Hall–MHD (2.1)–(2.4), their progressive decay is mediated by the non-ideal effects, such as the finite sound gyroradius term and nonlinear dissipative forces in the momentum equation that are predominant for the smaller scale density fluctuations.

A simulation shown in Fig. 3 depicts the evolution of the kinetic and magnetic energies for the parameters described in the caption. Owing to the equipartition between the magnetic and velocity fields, the latter can be replaced by the magnetic field in the expression of the diffusion coefficient to estimate the diffusive processes mediated essentially by field line (random) walk of magnetic field fluctuations, which govern the transport of energetic particles in the solar wind plasma.

Furthermore, it becomes evident from Fig. 3 that the effective diffusion of the plasma fluid is governed predominantly by the kinetic energy of solar wind turbulent fluctuations. Mode coupling interactions between the velocity and magnetic field fluctuations, amidst density perturbations, excite high-frequency and short length scale dispersive KAWs that are compressive and propagate along the direction of

https://doi.org/10.1017/S0022377810000486 Published online by Cambridge University Press

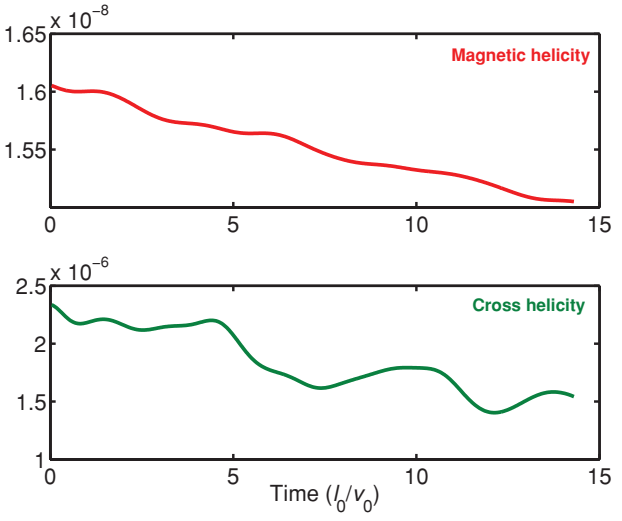


Figure 2. (Colour online) Evolution of the magnetic and kinetic helicities in 3D compressible Hall–MHD plasmas. Damping of the two is resulted by finite sound gyroradius effect. The simulation parameters are: spectral resolution is 128^3, $\eta = \mu = 10^{-3}, M_A = \beta = 1.0, kd_i \geqslant 1$, $L_x = L_y = L_z = 2\pi$.

the mean magnetic field B_0. While these waves must influence the local turbulent fluctuations in the inertial range, their role in the spectral energy cascades is not yet fully understood. We discuss this issue in the subsequent section.

4. Kinetic Alfvén inertial regime

The nonlinear spectral cascades in the KAW regime lead to a secondary inertial range in the vicinity of modes $kd_i \simeq 1$ in that the solar wind magnetic, velocity and field fluctuations follow turbulent spectra close to $k^{-7/3}$. This is shown in Fig. 4. The characteristic turbulent spectra in the KAW regime is steeper than that of the MHD inertial range which follows a $k^{-\alpha}$, where α is 5/3 or 3/2. The onset of the secondary inertial range is constantly debated because of the presence of multiple processes in the KAW regime that include, for instance, the dispersion, damping of EM ion-cyclotron waves, turbulent dissipation, etc. In the context of our simulations, the observed $k^{-7/3}$ in the solar wind turbulent plasma can be understood from the energy cascades affected by the Hall forces. The latter are one of the potential candidates that may be responsible for a $k^{-7/3}$ spectrum in the KAW inertial range regime.

To understand the observed $k^{-7/3}$ spectrum in the KAW inertial range regime in the solar wind plasma and in our simulations, we invoke the Kolmogorov and Kraichnan-like phenomenologies [10, 11] in the Hall–MHD plasma. The time scale associated with the Hall–MHD is $\tau_{\rm H}$, which is smaller than that of the MHD $\tau_{\rm MHD}$.

The nonlinear cascades in the MHD turbulence are governed typically by $\tau_{\rm MHD} \sim (ku_k)^{-1}$, where u_k is the velocity field in the k-space. By contrast, the spectral

https://doi.org/10.1017/S0022377810000486 Published online by Cambridge University Press

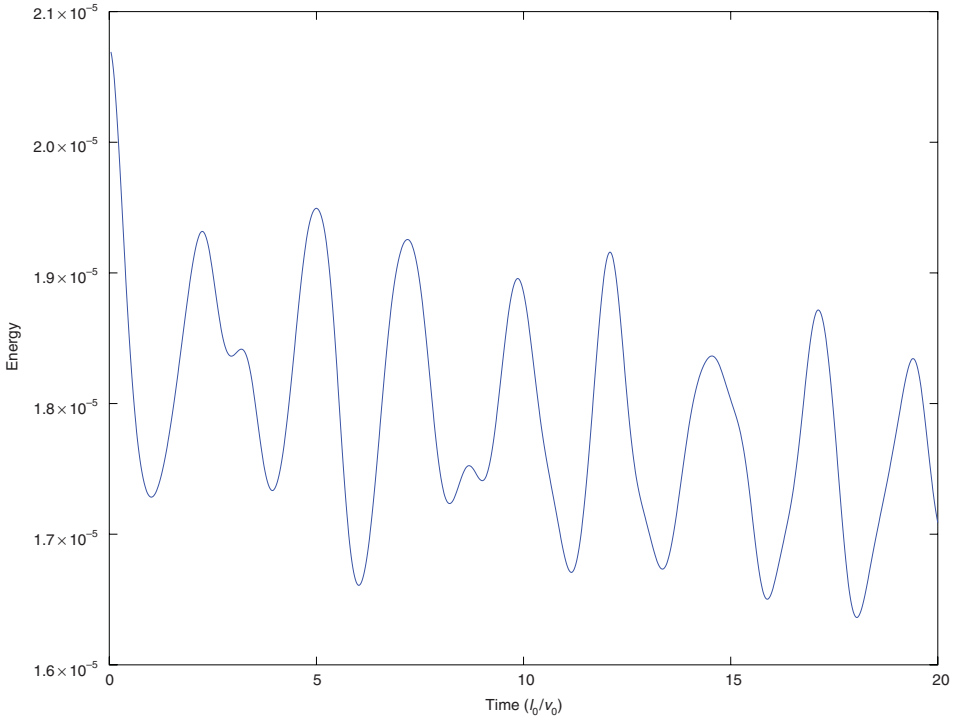


Figure 3. (Colour online) Evolution of the total (magnetic and kinetic) energy in 3D compressible Hall–MHD plasmas is shown. The corresponding turbulent transport χ_{eff} associated with velocity fluctuations is depicted by the lower curve. The simulation parameters are: spectral resolution is 128^3, $\eta = \mu = 10^{-3}, M_A = \beta = 1.0, kd_i \geqslant 1, L_x = L_y = L_z = 2\pi$.

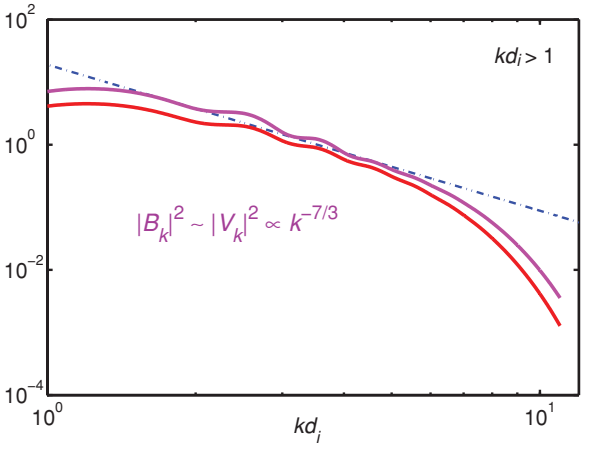


Figure 4. (Colour online) Inertial range turbulent spectra of the magnetic and velocity field fluctuations are shown along with that of the density fluctuation. These fluctuations closely follow a $k^{-7/3}$ spectrum in the kinetic Alfvén regime where $kd_i > 1$. Simulation parameters are the same as described in Fig. 3.

https://doi.org/10.1017/S0022377810000486 Published online by Cambridge University Press

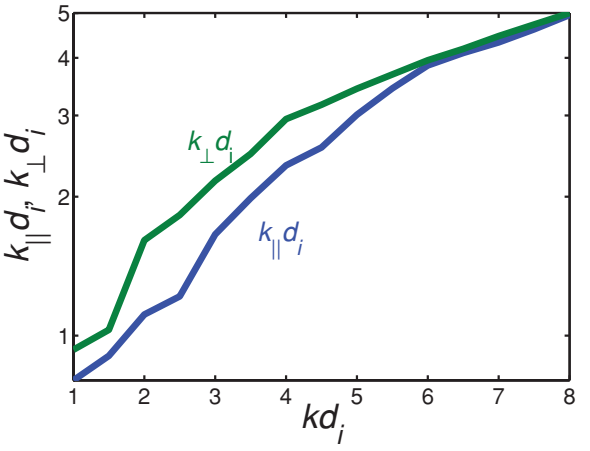


Figure 5. (Colour online) Spectrum of $k_\perp$ and $k_\parallel$ as a function of k. The large-scale inertial range turbulent fluctuations are more anisotropic as compared to the smaller ones.

transfer of the turbulent energy in the solar wind (Hall–MHD) plasma is $\tau_{\rm H} \sim (k^2 B_k)^{-1}$. The energy transfer rates in the KAW regime are, therefore, $\varepsilon \sim u_k^2/\tau_{\rm H}$. On substituting the turbulent equipartition relation between the velocity and magnetic fields $B_k^2 \sim u_k^2$, the energy transfer rates turn out to be $\varepsilon \sim k^2 B_k^3$. The use of the turbulent equipartition is justified from the observations and it is also seen in our 3D simulations (see Fig. 5). Applying the Kolmogorov's phenomenology [10, 11] that the energy cascades in the inertial range are local and that they depend on the Fourier modes and the energy dissipation rate, we obtain $k^{-1}B_k^2 \sim (B_k^3 k^2)^\alpha k^\beta$. Equating the indices of the common bases, we obtain $\alpha = 2/3$ and $\beta = -7/3$. This results in an energy spectrum $E_k \propto k^{-7/3}$ that is consistent with our 3D simulations (see Fig. 4) and the observations. On the other hand, the use of $\tau_{\rm MHD}$ in estimating the energy dissipation rates retrieves the inertial range MHD spectrum. This indicates that the Hall effects may be responsible for the spectral steepening in the solar wind plasma fluctuations in the $kd_i > 1$ regime. It is worth noted that our simulations in $kd_i < 1$ exhibit MHD-like $k^{-5/3}$ omnidirectional Kolmogorov-like [10] spectrum.

Moreover, the spectra given in Fig. 4 further shows a local anisotropy that is mediated primarily by the disparate spectral transfer processes in the inertial range solar wind plasma. It is confirmed in our simulations (not shown in figures) that both velocity and magnetic fields show strong signature of anisotropy in the spectral space. Furthermore, the turbulent anisotropy is more pronounced at the small-scale part of the spectrum.

5. Anisotropic cascades

To measure the degree of anisotropic cascades (or spectral anisotropy), we employ the following diagnostics to monitor the evolution of the $k_\perp$ mode in time. The averaged $k_\perp$ mode is determined by averaging over the entire turbulent spectrum

https://doi.org/10.1017/S0022377810000486 Published online by Cambridge University Press

weighted by $k_\perp$, thus

$$\langle k_\perp(t)\rangle = \left(\frac{\sum_k |k_\perp Q(k,t)|^2}{\sum_k |Q(k,t)|^2}\right)^{1/2}.$$

Here $\langle\cdots\rangle$ represents an average over the entire Fourier spectrum, $k_\perp = (k_x^2 + k_y^2)^{1/2}$ and Q represents any of $B, V, \rho, \nabla\times\mathbf{B}$ and $\nabla\times\mathbf{V}$. Similarly, the evolution of the $k_\parallel$ mode is determined by the relation,

$$\langle k_\parallel(t)\rangle = \left(\frac{\sum_k |k_\parallel Q(k,t)|^2}{\sum_k |Q(k,t)|^2}\right)^{1/2}.$$

It is clear from these expressions that the $\langle k_\perp(t)\rangle$ and $\langle k_\parallel(t)\rangle$ modes exhibit isotropy when $\langle k_\perp(t)\rangle \simeq \langle k_\parallel(t)\rangle$. Any deviation from this equality corresponds to spectral anisotropy. The scale-dependence of turbulent anisotropy is described in Fig. 4. Figure 4 shows discrepancy in $k_\perp$ and $k_\parallel$ is prominent at the smaller values of k. This essentially means that the large-scale turbulent fluctuations are more anisotropic than the smaller ones in a regime, where characteristic length scales are smaller than d_i, i.e. $kd_i > 1$. It further appears from Fig. 4 that the smaller scales in the $kd_i > 1$ are virtually *unaffected* by anisotropic KAWs that propagate along the externally imposed mean magnetic field B_0. Turbulent fluctuations with small characteristic scales in the $kd_i > 1$ regime of the Hall–MHD are not affected by the mean magnetic field or by KAWs. This leads us to conjecture that small-scale turbulence in the $kd_i > 1$ regime behaves essentially hydrodynamically, i.e. as eddies independent of the mean magnetic field or collisionless magnetized waves. Thus, large and smaller turbulent length scales evolve differently in the $kd_i > 1$ regime of the Hall–MHD turbulence.

6. Conclusion

In summary, we have explored nonlinear turbulent aspects of the Hall–MHD plasmas relevant to many space and astrophysical situations. In particular, we find that the EM turbulent fluctuations in $kd_i > 1$ regime exhibit a characteristic spectrum close to $-7/3$. This spectral index cannot be mediated by whistler wave processes, partly, because of the presence of the ion dynamics in our present two-fluid model. The inertial range in the $kd_i > 1$ regime exhibits significant anisotropy in velocity and magnetic field fluctuations through turbulent equipartition processes led essentially by the KAWs. The spectral properties of the Hall–MHD plasma, as described here, are relevant particularly to understand the observed solar wind and heliospheric turbulent processes.

Our future investigations shall include generalization of the present work to include the equilibrium density and magnetic field inhomogeneities so that the properties of coupled drift-Alfvén wave turbulence [29] can be studied to understand the anisotropic EM turbulence observed recently [18].

https://doi.org/10.1017/S0022377810000486 Published online by Cambridge University Press

Acknowledgements

The authors dedicate this paper to their esteemed colleague and friend Jose Tito Mendonça to honor him on the occasion of his 65th birthday. Tito is a classic physicist of our modern times and also a wonderful person we have come across during our scientific career.

This work was partially supported by NASA grants NNX09AB40G, NNX07AH18G, NNG05EC85C, NNX09AG63G, NNX08AJ21G, NNX09AB24G, NNX09AG29G, and NNX09AG62G, as well as by the Deutsche Forschungsgemeinschaft (Bonn) through project No. SH21/3-1 of the Research Unit 1048.

References

[1] Bhattacharjee, A. 2004 *Annu. Rev. Astron. Astrophys.* **42**, 365.
[2] Bhattacharjee, A., Ma, A., W. and Wang, X. 2001 *Phys. Plasmas* **8**, 1829.
[3] Biskamp, B., Schwarz, E. and Drake, J. F. 1996 *Phys. Rev. Lett.* **76**, 1264.
[4] Brodin, G. and Stenflo, L. 1990 *Contrib. Plasma Phys.* **30**, 413.
[5] Denskat, K. U., Beinroth, H. J. and Neubauer, F. M. 1983 *J. Geophys. Res.* **54**, 60.
[6] Ghosh, S., Siregar, E., Roberts, D. A. and Goldstein, M. L. 1996 *J. Geophys. Res.* **101**, 2493.
[7] Goldstein, M. L., Roberts, D. A. and Fitch, C. A. 1994 *J. Geophys. Res.* **99**, 11519.
[8] Goldstein, M. L., Roberts, D. A. and Matthaeus, W. H. 1995 *Astron. Astrophys.* **33**, 283.
[9] Howes, G. 2008 *Phys. Plasmas* **15**, 5904.
[10] Kolmogorov, A. N. 1941 *Dokl. Acad. Sci. URSS* **30**, 301.
[11] Kraichnan, R. H. 1965 *Phys. Fluids* **8**, 1385.
[12] Leamon, R. J., Matthaeus, W. H., Smith, C. W. and Wong, H. K. 1998 *Astrophys. J. Lett.* **507**, L181.
[13] Mahajan, S. and Krishan, V. 2005 Nonlin. *Process. Geophys.* **12**, 75.
[14] Marsch, E. 2006 *Living Rev. Solar Phys.* **3**, 1.
[15] Mendonça, J. T. and Shukla, P. K. 2007 *Phys. Plasmas* **14**, 122304.
[16] Mendonça, J. T., Serbeto, A., Davies, J. and Bingham, R. 2008 *Plasma Phys. Control. Fusion* **50**, 105009.
[17] Mendonça, J. T. and Rowlands, G. 1985 *Plasma Phys. Control. Fusion* **27**, 777.
[18] Narita, Y., Glassmeier, K.-H., Sahraoui, F. and Goldstein, M. L. 2010 *Phys. Rev. Lett.* 104, 171101.
[19] Shaikh, D. and Zank, G. P. 2003 *Astrophys. J.* **599**, 715.
[20] Shaikh, D. and Zank, G. P. 2005 *Phys. Plasmas* **12**, 122310.
[21] Shaikh, D. 2004 *Phys. Scr.* **69**, 216.
[22] Shaikh, D. 2009 *J. Plasma Phys.* **75**, 117.
[23] Shaikh, D. & Shukla, P. K. 2009 *Phys. Rev. Lett.* **102** 045004.
[24] Shaikh, D. & Zank, G. P. 2004 *ApJ.* **602**, 29.
[25] Shaikh, D. & Zank, G. P. 2006 *ApJ* **640**, 195.
[26] Shaikh, D. & Zank, G. P. 2007 *ApJ* **656**, 17.
[27] Smith, C. W., Isenberg, P. A., Matthaeus, W. H. and Richardson, J. D. 2006 *Astrophys. J.* **638**, 508.
[28] Shukla, P. K. 1978 *Nature* (London) **274**, 874.
[29] Sundkvist, D., Krasnoselskikh, V., Shukla, P. K., Vaivads, A., André, M., Buchert, S. and Rème, H. 2005 *Nature* (London) **436**, 825.

https://doi.org/10.1017/S0022377810000486 Published online by Cambridge University Press